Marine Geology 422 (2020) 106091

Contents lists available at ScienceDirect

Marine Geology

journal homepage: www.elsevier.com/locate/margo

Upper slope processes and seafloor ecosystems on the Sabrina continental slope, East Antarctica

A.L. Post[a,*], P.E. O'Brien[b], S. Edwards[c], A.G. Carroll[a], K. Malakoff[c], L.K. Armand[d]

[a] Geoscience Australia, GPO Box 378, Canberra, ACT 2601, Australia
[b] Macquarie University, Department of Environmental Sciences, NSW 2109, Australia
[c] Marine National Facility, CSIRO, Battery Point, TAS 7004, Australia
[d] Australian National University, Research School of Earth Sciences, Acton, ACT 2601, Australia

ARTICLE INFO

Editor: Michele Rebesco

Keywords:
Continental margin morphology
Southern Ocean
Multibeam bathymetry
Benthic biota
Biodiversity

ABSTRACT

This study applies detailed seafloor bathymetry data and seafloor images to understand upper slope features and how these influence the distribution of seafloor biota on the East Antarctic margin. The East Antarctic slope on the Sabrina margin has been shaped by diverse processes related to repeated glaciation. Differences in the morphology of gullies on the upper slope enable an understanding of the likely processes that have been active on this margin. Gully morphology varies according to changes in slope gradient, which may have driven variations in sedimentation. Areas of lower slope angles may have led to rapid sediment deposition during glacial expansion to the shelf edge, and subsequent sediment failure. Typically, gullies in these areas are U-shaped, initiate well below the shelf break, are relatively straight and long, and have low incision depths, consistent with formation due to mass wastage. Areas of higher slope angles likely experienced enhanced flow of erosive turbidity currents during glaciations associated with the release of sediment-laden basal meltwaters. Sediment-laden subglacial meltwater flows typically create gullies such as those we observe that initiate at, or near, the shelf break; are V-shaped in profile; and have high sinuosity, deep incision depths and a relatively short downslope extent. The short downslope extent reflects a reduced sediment load associated with increased seawater entrainment as the slope becomes more concave in profile. These differences in gully morphology have important habitat implications associated with differences in the composition and beta-diversity of the seafloor communities. This upper slope region also supports seafloor communities that are distinct from those on the adjacent shelf, highlighting the uniqueness of this environment for biodiversity. Conservation strategies therefore need to consider slope and shelf communities as distinct and equally important components of the Antarctic ecosystem.

1. Introduction

Upper continental slope regions on glacial margins are dynamic, steep areas of the seafloor, often intersected by gullies and canyons. The morphology and sedimentation on the continental slope preserve the history of past ice dynamics on these margins. During late Cenozoic glaciations, the expansion of ice sheets across the Antarctic continental shelves resulted in the erosion of major shelf troughs (Anderson et al., 2002; Livingstone et al., 2012). Where ice sheets expanded across sedimentary substrates, large volumes of sediments were eroded and entrained into the base of the ice sheet (Ó Cofaigh et al., 2003). These sediments were subsequently deposited down the continental slope. On steep continental slopes (> 10°) sediment is more likely to be transferred rapidly downslope in debris and turbidity flows, eroding extensive networks of gullies and canyons (Dowdeswell et al., 2004; Ó Cofaigh et al., 2003). Lower slopes (generally < 10°) reflect deposition of large volumes of unstable sediment from ice grounded at the shelf edge. Iceberg turbation, during present and past interglacial periods, resuspends glacial and glacimarine sediments along the outer continental shelf, producing dense turbid downslope flows (Barnes and Lien, 1988; Gales et al., 2014; Prothro et al., 2018). The dense waters produced in shelf polynyas can also flow down the continental slope (Amblas and Dowdeswell, 2018), and may assist in flushing upper slope gullies and canyons (e.g. Dowdeswell et al., 2008; Dowdeswell et al., 2006; Kuvaas and Kristoffersen, 1991; Noormets et al., 2009).

Spatial variability in continental slope morphology, including the characteristics of upper slope gullies, reflect differences in past ice dynamics and the subsequent delivery of sediment to the margin. The

* Corresponding author.
E-mail address: alix.post@ga.gov.au (A.L. Post).

https://doi.org/10.1016/j.margeo.2019.106091
Received 7 August 2019; Received in revised form 21 November 2019; Accepted 26 November 2019
Available online 29 November 2019

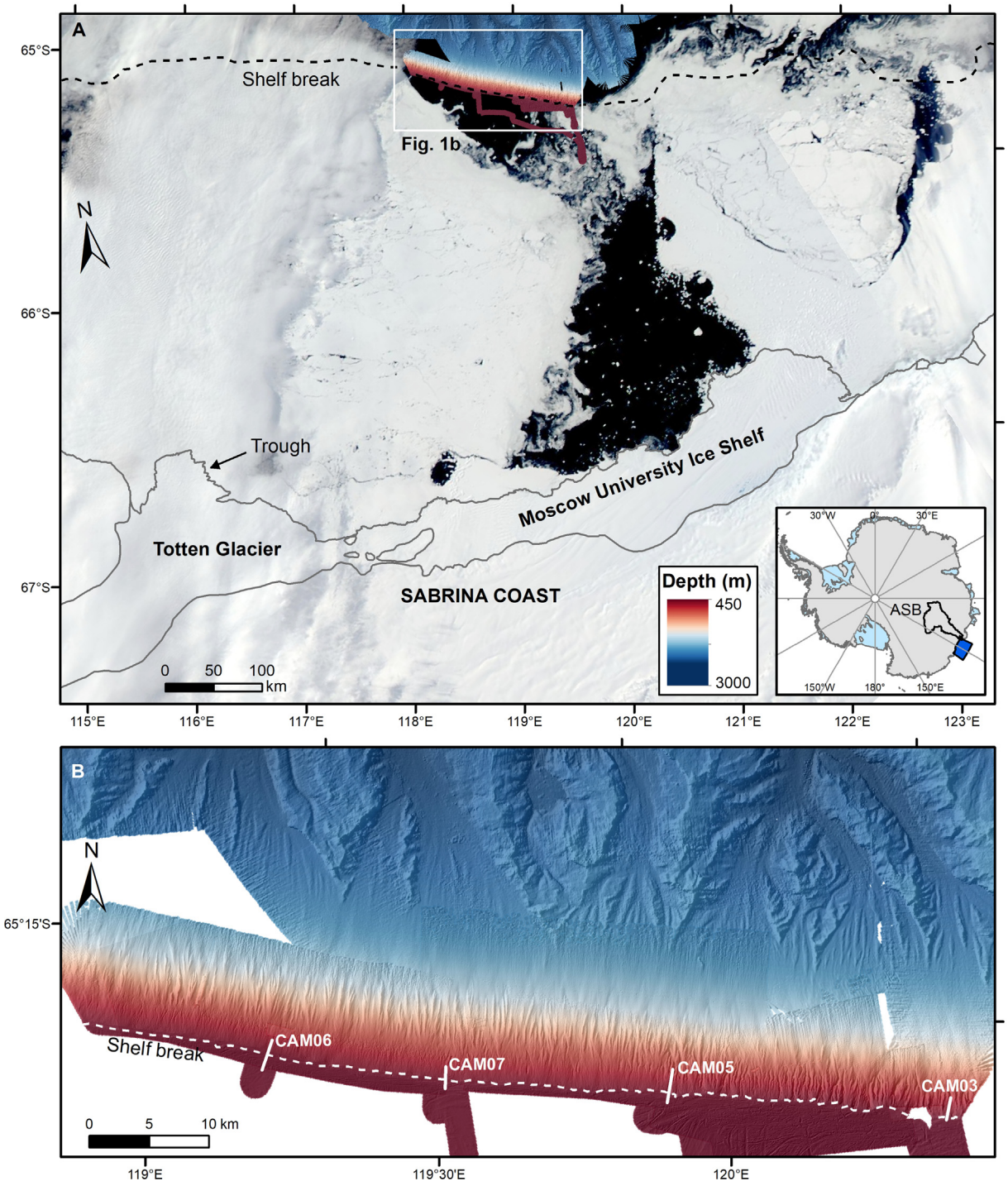

Fig. 1. A) Location of study area showing sea ice conditions from the MODIS satellite on 17 February 2017. The arrow indicates the location of a deep trough identified by Silvano et al., 2017. The inset shows the location of the Aurora Sub-Basin (ASB) and a proposed MPA (blue rectangle) that overlaps with the study area. B) Upper slope bathymetry data with overlapping grids from shallower to deeper at 10 m (EM710), 25 m and 50 m resolution (EM122). Locations of camera transects are also shown (white lines). Dense iceberg scouring is visible on the outer shelf, gullies are present at depths below the shelf break, and canyons occur on the lower slope. For full bathymetry dataset refer to O'Brien et al., (in review). (For interpretation of the references to colour in this figure legend, the reader is referred to the web version of this article.)

upper slope, across most of the East Antarctic margin, has slope values of 5–15°, with localised areas up to 20°, while parts of the West Antarctic margin, such as off Marie Byrd Land and the West Antarctic Peninsula, reach slope angles up to 26° (Arndt et al., 2013). Turbidity currents generated from sediment-laden subglacial meltwater are the most widespread mechanism for gully formation around the Antarctic margin, with evidence for gully generation from small-scale slides also observed (Gales et al., 2013).

In this study, we use multibeam echosounder data and sub-bottom profiles to assess the morphology of the upper slope, and interpret gully characteristics in the context of past and present processes that have shaped the Sabrina continental margin, offshore from the Totten Glacier and Moscow University Ice Shelf (Fig. 1). Details of the glacial and oceanographic processes that have shaped the lower slope are

provided in a companion paper by O'Brien et al., n.d.. Aerogeophysical data indicate that the Totten Glacier has repeatedly advanced and retreated over at least the past 7 Ma, eroding deep subglacial basins beneath the ice sheet (Aitken et al., 2016). Marine geophysics and sediment cores on the shelf indicate the establishment of marine-terminating glaciers by the early to mid-Eocene (Gulick et al., 2017), with evidence suggesting that the ice sheet has expanded to within ~5 km of the shelf break during past glaciations (Fernandez et al., 2018). Gullies mapped from a small area of the upper slope adjacent to the grounding line promontory are interpreted to have formed from sediment-laden meltwater discharged from the base of the expanded ice sheet (Fernandez et al., 2018).

This study also uses towed underwater imagery to assess the distribution of seafloor biota on the upper slope of the Sabrina continental margin. The composition of upper slope ecosystems on the Antarctic margin is poorly known, as many parts of the upper slope are difficult to access due to persistent sea ice cover. Upper slope ecosystems are influenced by a range of oceanographic and sedimentary processes (Neal et al., 2018; Post et al., 2010; Thatje et al., 2005). Understanding these ecosystems can aid our interpretation of how benthic biota respond in a dynamic environment. This study examines whether gully type, and associated sedimentary processes, influence the distribution and abundance of seafloor biota across the upper slope off the Sabrina Coast, and whether upper slope communities are distinct from those on the adjacent continental shelf (Post et al., 2017). The data and interpretations from this study provide a baseline for understanding and monitoring an area nominated as a potential Marine Protected Area by Australia and the European Union.

2. Physical and Oceanographic setting

The Sabrina upper slope region is offshore from the Totten Glacier and Moscow University Ice Shelves, both of which drain extensive and deep ice in the interior of East Antarctica (Aitken et al., 2016; Young et al., 2011). The Totten Glacier and the Moscow University Ice Shelf lie at the seaward end of the Sabrina subglacial Basin, which connects to the Aurora Sub-basin further inland (Fig. 1). The East Antarctic Ice Sheet has expanded repeatedly across the continental shelf to the slope through the Totten Glacier and Moscow University Ice Shelf (Fernandez et al., 2018; Gulick et al., 2017).

The Antarctic continental slope is typically swept by a westward flowing bottom current, the Antarctic Slope Current, associated with the sub-surface Antarctic Slope Front (ASF) (Williams et al., 2011). The ASF separates low density Antarctic Surface Water from relatively dense modified Circumpolar Deepwater (mCDW) (Bindoff et al., 2000). On the Sabrina upper slope the ASF occurs inshore of the shelf break with mCDW present over the shelf break and downslope to ~1200 m. The intrusion of mCDW onto the shelf break and upper slope region appears to be persistent on an annual and interannual basis (Nitsche et al., 2017; Williams et al., 2011). The presence of mCDW is significant for marine ecosystems in that it supplies nutrients that drives primary productivity in the surface layers (Williams et al., 2011). On other parts of the Antarctic margin, downslope flow of Antarctic Bottom Water generated in shelf polynyas can also supply food to seafloor slope communities (Jansen et al., 2018). The Dalton Ice Tongue Polynya is a recurrent latent-heat polynya west of the Moscow University Ice Shelf (Massom et al., 1998), but there is no evidence to suggest that sufficient dense shelf water is generated from this polynya to form Antarctic Bottom Water (Williams et al., 2011).

3. Methods

3.1. Geophysical data collection

Multibeam bathymetry was collected on the RV *Investigator* during voyage IN2017_V01 in January to March 2017. Data were collected using hull-mounted Kongsberg EM122 and EM710-Mk2 echosounders. The EM122 is a 12 kHz full ocean depth echosounder with a 1 × 1° array and was operated at all water depths during the Sabrina Seafloor Survey. The EM710-Mk2 has transmission frequencies between 40 and 100 kHz with a 0.5 × 1° array, and mapped depths up to 2000 m on the continental shelf and upper slope. The final surface from the EM122 was gridded at resolutions of 25 m and 50 m for the upper slope region and 200 m for the whole survey area, while the EM710 data on the shelf and upper slope was gridded to 10 m (Fig. 1). Broad and small-scale rugosity were calculated based on the 200 m and 25 m bathymetry grids respectively using the Benthic Terrain Model toolbox in ArcGIS (Wright et al. 2012). Backscatter mosaics were produced with a 20 m resolution for the EM122 and 5 m resolution for the EM710 sonar. Mosaics were constructed with automated processing within the Fledermaus Geocoder Toolbox (for further details see Armand et al., 2018).

Sub-bottom profile data were acquired throughout the survey with a Kongsberg SBP120. The system source was a linear chirp sweep of 2.5–6.5 kHz with a pulse length of 6 milliseconds. The system operated in single ping mode in the shallower depths of the upper slope. The data were recorded as two-way time sections.

3.2. Gully parameters

Upper slope gullies were mapped using the ArcGIS hydrology toolbox. Gullies were then edited manually to include only those with an incision depth of > 2 m, retaining 850 gully segments/branches and a total number of gully networks of 160 gullies. Gullies were mapped as far downslope as they could be traced in a consistent manner while retaining a > 2 m incision depth. Gully parameters were extracted to determine width and incision depth at the head of each gully segment/branch, total and segment length, sinuosity (see Eq. (1)) and cross-sectional shape (Eq. (2)). Length was also measured as the total linear extent downslope. Width was measured between points of maximum curvature. A small number of length measurements (1%) were limited by the data coverage for the upper parts of the gullies, and therefore represent minimum lengths.

$$Sinuosity = \frac{distance\ along\ gully}{straight\ line\ distance} \quad (1)$$

Segments with sinuosity values > 1.04 were considered to be sinuous, while those < 1.04 were classified as straight (Gales et al., 2013). While measurements were undertaken on all gully segments/branches, the analysis here focusses specifically on the characteristics of first-order gullies, defined using Strahler stream order (Strahler, 1957).

The cross-sectional shape of each gully was measured between points of maximum curvature, just below the top of each gully segment/branch and parallel to the shelf break. Shape was calculated using the General Power Law program (Pattyn and Van Huele, 1998), which distinguishes between gullies ranging from V-shaped ($b = 1$) to parabolic or U-shaped ($b = 2$) according to Eq. (2). A value $b < 1$ indicates a convex-upward slope, while $b > 2$ reflects a more box-shaped profile. A value of 1.5 was used as a cut-off between U and V-shaped gullies. The program calculates the cross-sectional shape (b) by determining the minimum RMS between the observed cross-section and a large set of symmetrical shapes defined by Eq. (2). In Eq. (2) a and b are constants, χ and y are the horizontal and vertical coordinates taken from the cross-sectional profile and χ_0 and y_0 are the coordinates at the origin of the profile.

$$y - y_0 = a\ |\chi - \chi_0|^b \quad (2)$$

3.3. Seafloor images

Four camera tow transects were completed on the upper slope

Table 1
Details of camera tow transects. Positions and pressures are shown for the towed body based on USBL and CTD data, with pressure (dBar) to depth (m) conversions based on Fofonoff and Millard (1983). SOL = Start of Line, EOL = End of Line.

Transect	Latitude	Longitude	Pressure	Depth	No. images analysed
C26_CAM03_SOL	−65.5595	120.3877	501	496	49
C26_CAM03_EOL	−65.5494	120.3993	723	714	
C28_CAM05_SOL	−65.4918	119.9197	503	498	52
C28_CAM05_EOL	−65.4807	119.9320	732	723	
C32_CAM06_SOL	−65.3847	119.2552	500	495	49
C32_CAM06_EOL	−65.3753	119.2708	680	672	
C36_CAM07_SOL	−65.4410	119.5444	498	493	53
C36_CAM07_EOL	−65.4282	119.5537	708	700	

during survey IN2017_V01 using the Marine National Facility's Deep Tow Camera (Fig. 1). This system collected oblique facing still images every 5 s with a Canon – 1DX camera, and high definition video with a Canon – C300 system. Four SeaLite Sphere lights provided illumination and two parallel laser beams (10 cm apart) provided a reference scale for the images. This study presents results from the analysis of the still imagery acquired during IN2017_V01. All camera tows were run at a ship speed of approximately 2 knots over the seafloor, enabling a spacing between still images of ~5 m. Several sensors were attached to the towed body, including a SBE 37 CTD for collection of salinity, temperature and pressure data, a Kongsberg Mesotech 1007D altimeter and a Sonardynne beacon to record the location of the towed system. Unfortunately, altimeter data could not be used due to timing offsets that were not able to be resolved. Transects were run downslope from the continental shelf break to reduce the risk of colliding with the seafloor. Images were analysed over a depth range of ~495 m to 670–725 m, with 49–53 images analysed for each transect (for details see Table 1). All colour-corrected imagery is archived via THREDDS (http://dapds00.nci.org.au/thredds/catalog/fk1/IN2017_V01_Sabrina_Seafloor/catalog.html).

3.4. Analysis of seafloor images

All images were constrained to a depth range of 495–725 m prior to analysis and assessed to remove those that were too blurry, and those that were too far from, or too close, to the seafloor for analysis. Distance to the seafloor was assessed based on the ratio of the distance between the laser pointers to the width of the computer screen, with the ratio for good images between 0.018:1 and 0.064:1 (D. Osterhage, pers. comm.), equivalent to imaging an area of seafloor of between 2 and 15 m^2. Biota and substrates were characterised for every fifth image according to the CATAMI image classification scheme (Collaborative and Automated Tools for Analysis of Marine Imagery, Althaus et al., 2015) and consistent with national standard operating procedures (Carroll et al., 2018). Images were uploaded into the online platform SQUIDLE+ (a web-based interface for the management, exploration and analysis of seafloor imagery: http://squidle.org/) for analysis. Biota were counted as presence/absence of all visible biota for each image. Quantitative counts were not attempted due to variable image quality and oblique image angles, which would have led to inconsistencies in abundance data. Percent biological cover and substrate type for the whole image was calculated based on analysis of 30 random points across each image. For each point, the presence/absence of biota was classified as well as the substrate type as sand/mud, gravel, pebble, cobble or boulders. Percent cover calculations were standardised according to the proportion of scored points on each image, excluding those that were too dark to classify. A total of 203 images were analysed. All image annotations are archived through the Australian Antarctic Data Centre (Post et al., 2019).

3.5. Statistical analysis of seafloor communities

Statistical analyses to understand variations in community composition with respect to environmental gradients were implemented in the PRIMER 7.0 package. The similarity between samples based on the taxa composition was determined using the Jaccard coefficient, appropriate for analysis of presence-absence data (Clarke et al., 2014). Similarities between images were visualised using non-metric multidimensional scale (nMDS) plots. The ANOSIM (analysis of similarities) function was used to test the null hypothesis that there were no significant differences in the composition of taxa between transects, with a permutation test (n = 9999 permutations) to determine the significance of any differences between transects. PERMDISP was used to test for changes in variability in community structure between transects by measuring and comparing the distance from observations to the centroid of each group (Anderson et al., 2006). This function provides a measure of beta-diversity, which indicates difference in the species diversity for a local area relative to the regional species pool (Whittaker, 1960; Whittaker, 1972). A permutation test (n = 9999 permutations) provided a measure of statistical significance for differences in community structure between transects.

4. Results

4.1. Outer shelf features

Multibeam bathymetry data from the outer shelf revealed features indicative of former grounding of the ice sheet near the shelf break (Fig. 2). North-westerly orientated ridges were mapped across the outer shelf margin (see arrows on Fig. 2). These ridges were ~5 m high, symmetrical and extended laterally beyond our data. A second, more recent set of ridges was also observed, with a more westerly orientation. Sub-bottom profiles indicated that the ridges were comprised of an acoustically semi-transparent sedimentary unit, overlying a smooth basal reflector. There was a broad (~5 km wide) grounding zone wedge (GZW) within ~2 km of the shelf break, forming a 20–30 m high ridge.

4.2. Diversity and characteristics of gullies

The Sabrina upper slope was heavily dissected by gullies (Fig. 3), initiating either at, or just below, the shelf break, with the shelf break occurring at depths of 460–530 m. Gullies formed branching stream networks right along this upper slope region and extended downslope to depths of 1000–2200 m. At ~2000 m the seafloor became smooth, and had a lower gradient (~7°). Larger canyons initiated at ~2500 m. From east to west across the upper slope, gullies initiated and finished at progressively deeper water depths. Most gullies at the eastern end, cut the shelf break and extended to 1000 to 1600 m depth (Fig. 3c), while in the west, gullies initiated at ~650 m and ended at 1800 to 2200 m (Fig. 3b).

Other gully attributes indicated a general divide between the eastern and western parts of the upper slope area, particularly between depths of ~550 m and 900–1000 m. Based on the change in gully morphology, the upper slope region was broadly divided at ~120°E, with areas > 120°E referred to here as east, and those < 120°E referred to as west. First-order gullies on the eastern side tended to be more sinuous, wider and deeper than gullies to the west (Table 2). Histogram plots indicated a much larger range in the parameter characteristics across eastern gullies, despite a significantly lower number of gullies (Figs. 3 and 4). The cross-sectional shape of the gullies had a variable distribution between west and east (Fig. 5). Groupings of V-shaped gullies in the east were interspersed by groups of slightly U-shaped gullies. In contrast, the central to western parts of the region were mostly U-shaped with extreme U-shape values for many gullies, but some V-shaped gullies also present (Figs. 4 and 5). As a consequence, the histogram plot indicated a much larger range in cross-section values

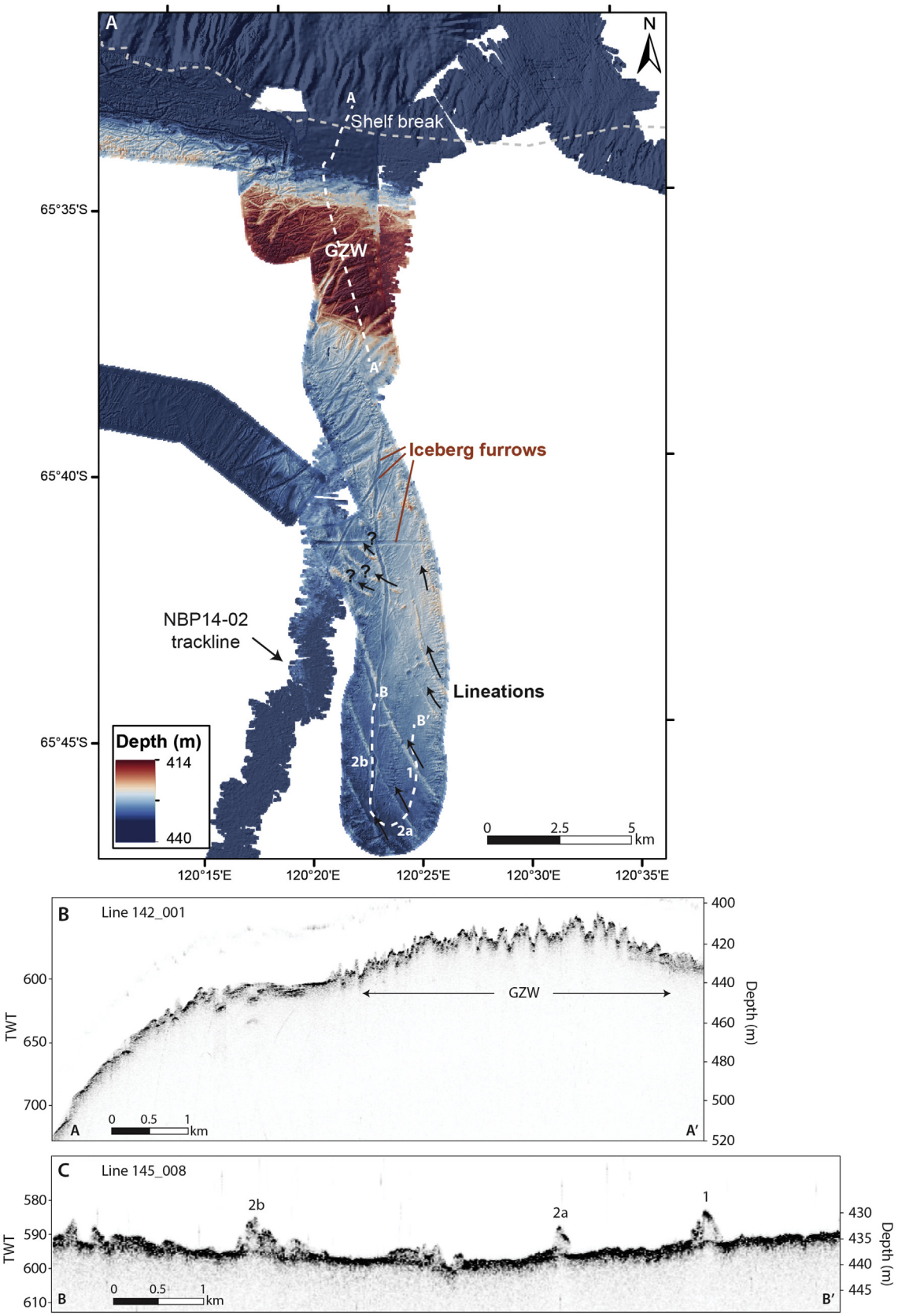

Fig. 2. A) Glacial advance features, including a grounding zone wedge (GZW) and glacial lineations, indicative of grounding near the shelf break. Arrows indicate former ice flow direction based on ridge orientation. Multibeam data from *Nathaniel B. Palmer* voyage NPB14–02 also shown (see Fernandez et al., 2018). B) Sub-bottom profile (A to A') over GZW on the outer shelf. The seafloor has subsequently been heavily impacted by iceberg scours. C) Profile across glacial lineations (B to B′), showing ridges of semi-transparent sediment unit overlying a smooth basal reflector. Lineations are numbered as shown on the transect in A.

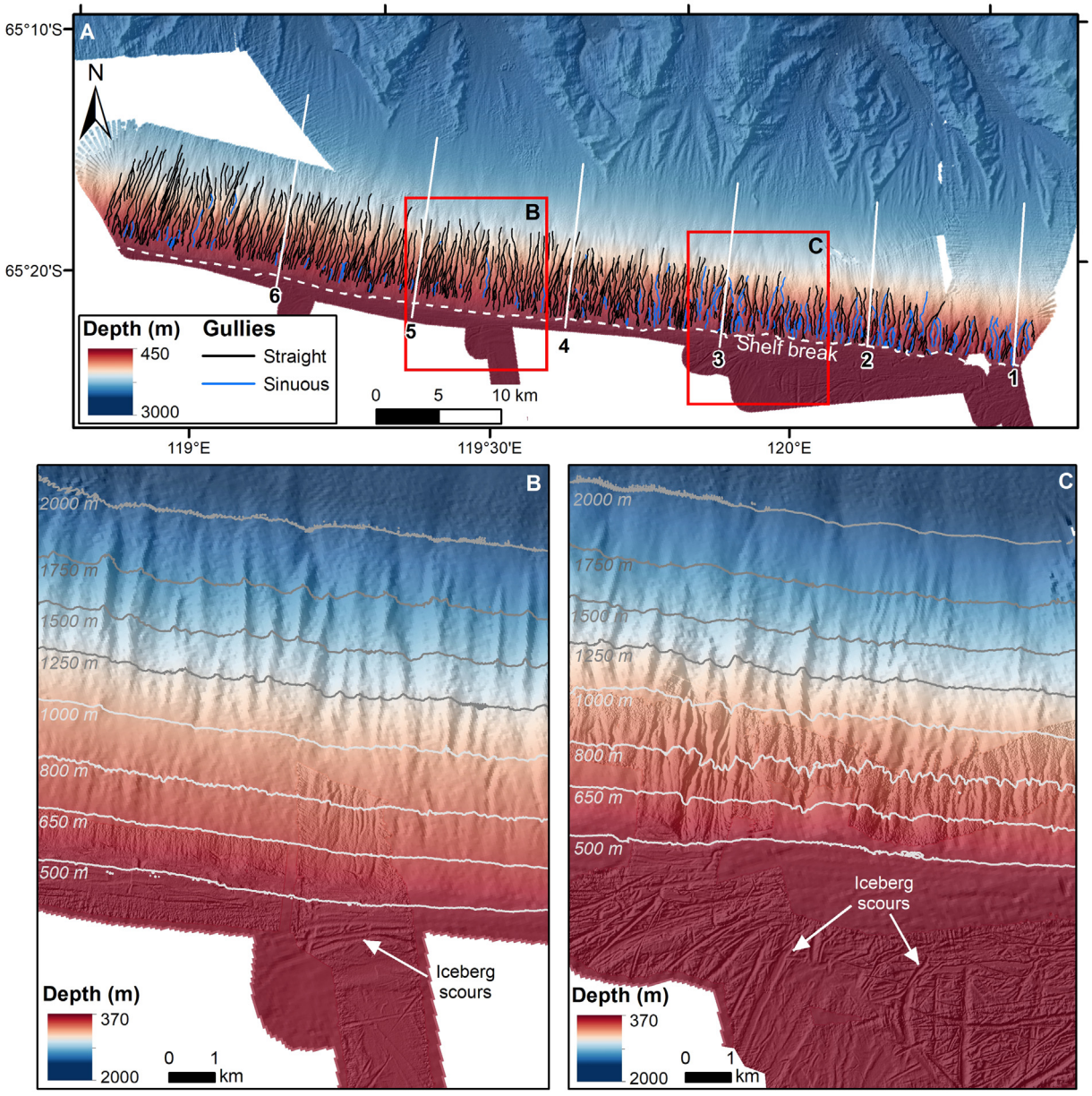

Fig. 3. A) Upper slope gullies on the Sabrina seafloor, coloured as sinuous and straight. Lines refer to transects shown on Fig. 6. B) Western and C) Eastern insets showing bathymetry over contours for reference. On the outer shelf and upper slope, insets show available multibeam echosounder data from the EM710 (10 m resolution) overlain on EM122 multibeam echosounder data (50 m resolution). Iceberg scours imaged on the outer shelf are highlighted.

Table 2
Gully properties for first-order gullies and slope values from the shelf break to 1000 m between eastern (> 120°E) and western sectors (< 120°E). Note that gully length is the total linear length of gullies.

	Average (± 1 s.d.)		Min		Max	
	East	West	East	West	East	West
Width (m)	84.5 ± 59.1	109.5 ± 81.1	1.2	6.2	428.0	396.0
Incision depth (m)	5.6 ± 5.4	8.3 ± 7.2	2.0	2.0	61.5	46.0
Cross-section shape	1.9 ± 1.5	1.4 ± 0.5	0.7	0.6	12.2	3.7
Sinuosity	1.02 ± 0.02	1.04 ± 0.03	1.00	1.00	1.11	1.14
Gully length (m)	3305 ± 1078	4729 ± 1841	686	56	4861	8048
Slope (°)	13.0 ± 4.8	9.6 ± 2.6	2.0	3.5	58.9	40.2

for the western than eastern gullies.

The gradient of the continental slope also varied between the eastern and western parts. On the eastern side, the uppermost slope was typically steep (average slope 13.0° ± 4.8) and rugged compared to the smoother, shallower slopes of the western side (average slope 9.6° ± 2.6) (Table 2). Below 1000 m, slope gradients were similar between the east and west (average 10.3° ± 1.4). Profiles indicated that the uppermost slope (to 1000 m) had a fairly constant slope, whereas below 1000 m the slope became concave in profile (Fig. 6). The profiles also indicated a lengthening of gullies from east to west. Gullies in the east extend downslope for 8 km (profile 1), with a gradual extension in length to 17 km in the west (profile 6). Eastern gullies tended to terminate as slopes increased (profile 1), whereas to the west (profiles 2–6), gullies continued through this steeper region.

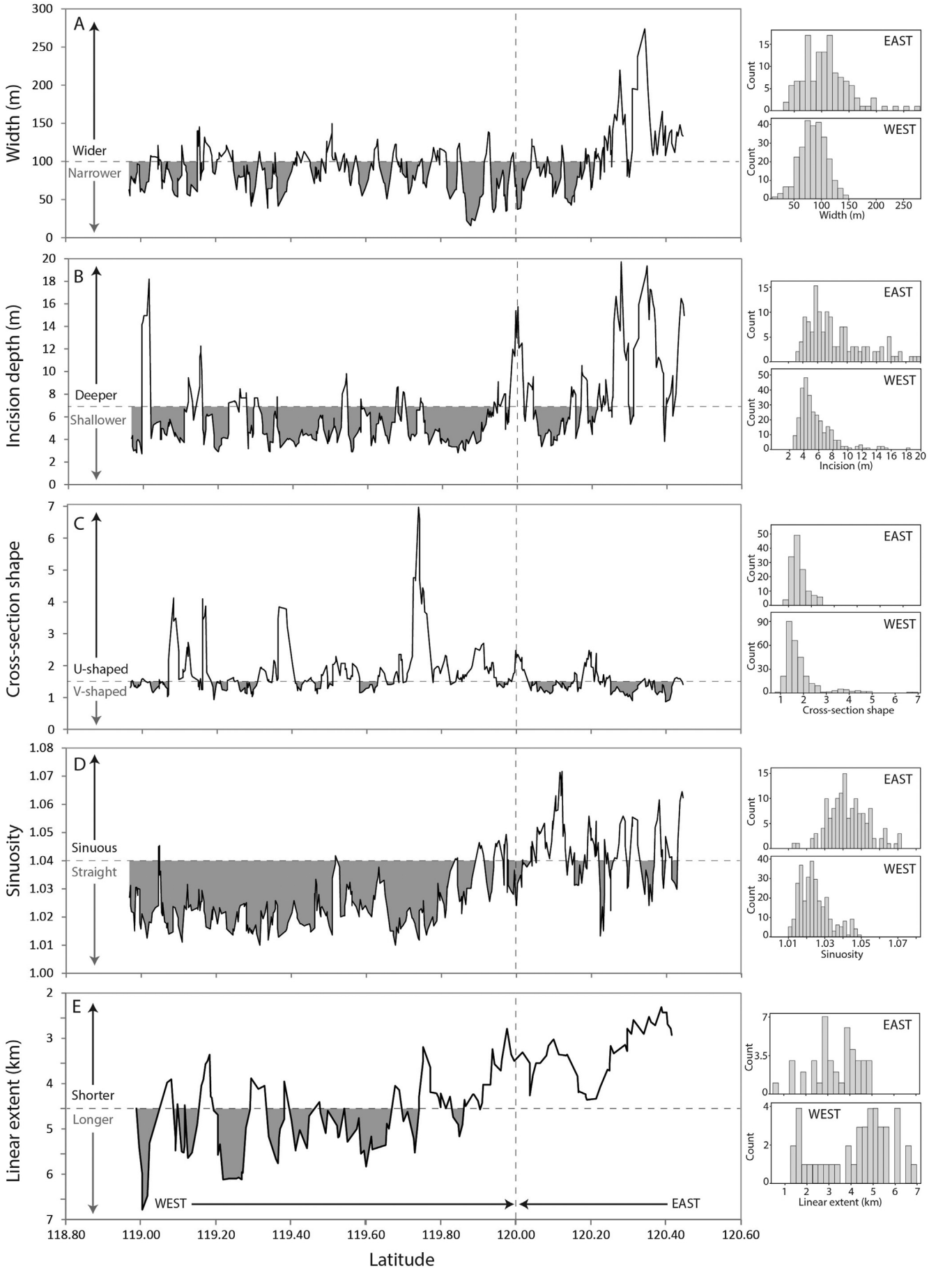

(caption on next page)

Fig. 4. 5-point moving averages from first-order gullies showing from west to east gully width (A), incision depth (B), cross-section shape (C), sinuosity (D) and total linear extent (E). Histograms show the distribution of values in the eastern and western sectors, with the extent of these zones shown in E. A distinct divide is observed for all gully properties, apart from the cross-section shape, between the western and eastern sectors.

4.3. Gully substrates from backscatter data

The nature of the substrate within the gullies was assessed based on multibeam backscatter data, however, due to variable quality of the backscatter data, gullies could only be resolved in a few locations (Fig. 7). In these areas gully thalwegs had generally higher backscatter values, implying they were harder than surrounding areas of the seafloor, particularly in Area A. Area B showed a more variable backscatter response, with many gully thalwegs having high backscatter, while some lower backscatter gullies were also apparent, implying soft-floors.

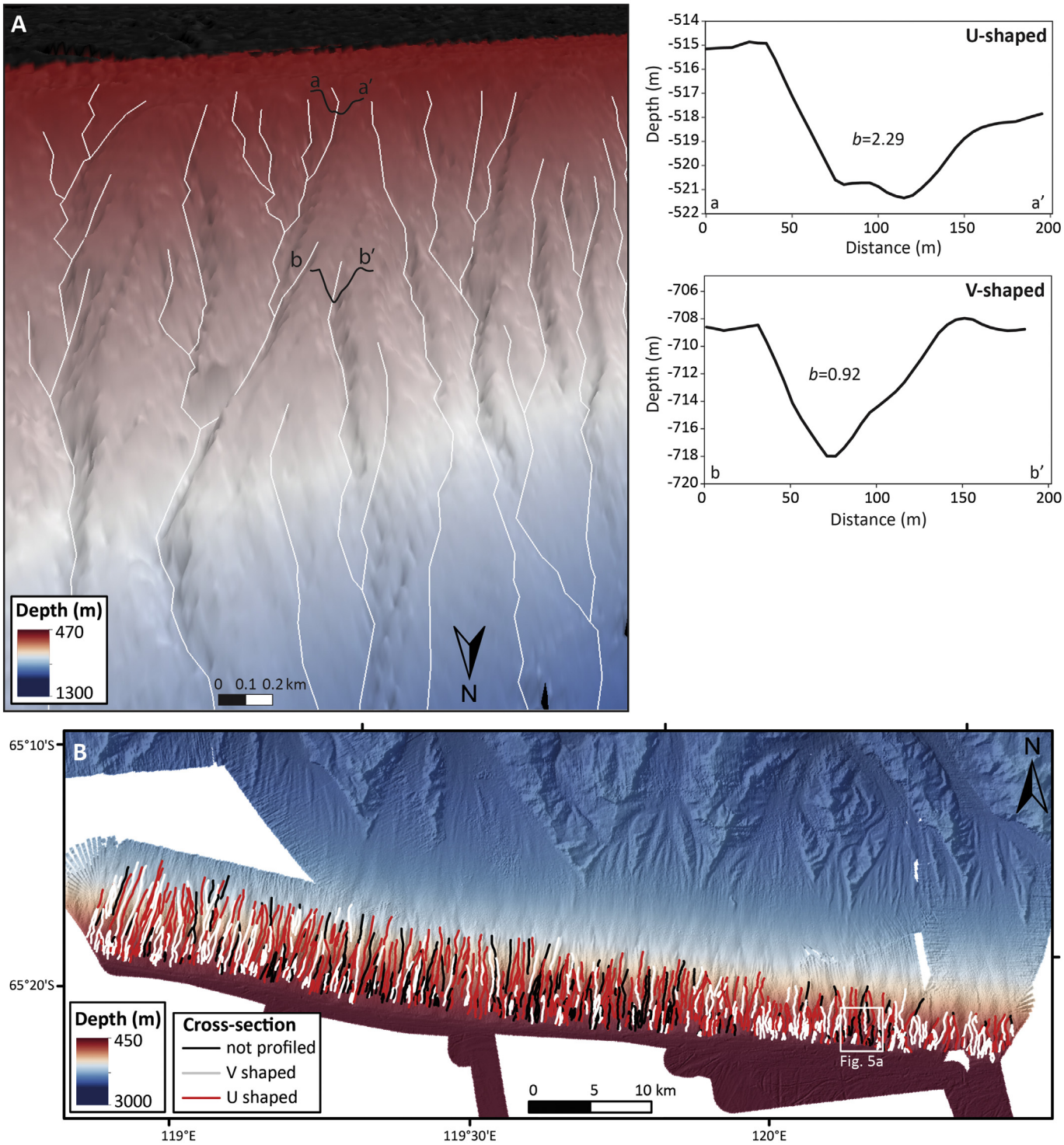

Fig. 5. Gully cross-sections (a) detailed 3D view of U-shaped and V-shaped gullies, with profiles and *b* coefficient values from across each type; (b) distribution of V- and U-shaped gullies along the upper slope. Note that some gullies were too small at the resolution of the data to be accurately profiled.

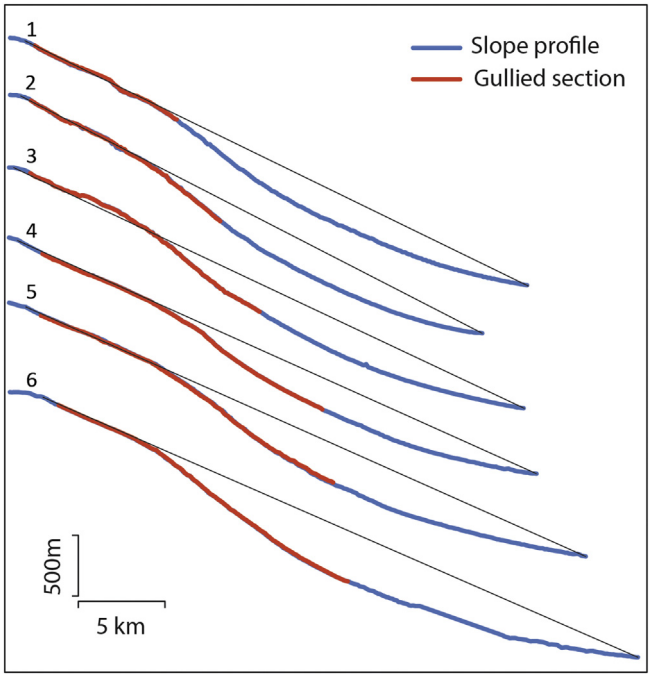

Fig. 6. Slope profiles from east to west, from the shelf break (~500 m) to 2500 m. Black lines provide a guide for viewing profile shape from the shelf break to the base of each section. Red lines indicate the extent of gullies on each profile. For locations of profiles refer to Fig. 3. (For interpretation of the references to colour in this figure legend, the reader is referred to the web version of this article.)

4.4. Nature of seafloor communities

The seafloor communities observed on the Sabrina slope had fairly consistent diversity (36 to 39 taxa were observed on each transect), though with variable abundance of organisms. Percent cover ranged from 0 to 77%. Highest average percent cover was observed on transect CAM05 (28%), and much lower percent cover (14–17%) on the other three transects. Brittle stars and polychaete tubeworms were almost ubiquitous in all images, and anemones were frequently observed (Fig. 8). Transects CAM06 and CAM07 contained a high number of octocorals, primarily *Thourella* sp., classified as a simple bottle-brush morphology in the CATAMI classification (CAAB code 11 168906). A variety of sponges, urchins, bryozoans, holothurians, bivalves and solitary corals were also widespread. A few taxa had locally high abundances, including the urchin *Sterichinus* sp. and bushy gorgonians.

Differences between transects were tested with an analysis of similarity (ANOSIM), which indicated a significant difference (Global $R = 0.207$; $p < .02$) in the composition of the biota between each transect. Closest similarity was found between transects CAM06 and CAM07 in the western part of the slope, while CAM03 in the east showed the greatest dissimilarity to the other transects (Fig. 9b). The overlap in taxa composition among transects is illustrated by the MDS plot (Fig. 9a), which also reveals differences in the distribution of points. Transects CAM03 and CAM05 had a broader distribution of points than the other two transects, indicating a wider variation in the composition of the taxa. These differences in dispersion were quantified by the PERMDISP analysis (Fig. 9c). Pairwise comparisons between each transect indicated a significant difference in dispersion based on taxa composition among all transects, apart from between transects CAM06 and CAM05 and CAM07 and CAM05 (Table 3). There was also a significant overall difference in dispersion between the eastern rugged (CAM03 and 05) and western smooth (CAM06 and 07) gully types ($p = .0001$).

Environmental attributes varied between towed camera transects, with differences in sediment texture and broad- and small-scale rugosity (Fig. 10). Transect CAM05 had the highest small- and broad-scale rugosity and the most common hard substrates, with average cover by boulders and cobbles of 13%, and over 50% in some images. Transect CAM03, by contrast, had the highest cover of soft sediments, with the quartile range for mud and sand ranging from 65 to 95%. CAM03 also had high broad-scale rugosity, with rugged gullies occurring around this transect.

Tests of the association between community composition and environmental attributes did not reveal any strong environmental drivers, however, significant differences in community composition were found between the more rugged gullies to the east and the smoother gullies to the west. The difference in community structure between these areas was best illustrated by the changes in the dispersion of taxa, or the beta-diversity. There was progressively less variation in community composition from east to west (Fig. 9c). The ANOSIM analysis also indicated that the two transects from the western smoother canyons (CAM06 and CAM07) were significantly more similar to each other than to the rugged canyons in the east (Fig. 9b). These results indicated a subtle, but significant, difference in the nature of the seafloor communities between the gully types identified.

4.5. Comparison between shelf and slope communities

To enable a comparison between shelf and slope communities, the data collected on the slope was compared to a previous analysis from the adjacent shelf (Post et al., 2017). Shelf taxa abundance data were converted to presence-absence data and restricted to a depth range of 495–725 m (leaving 225 images) for comparison to the upper slope communities presented here. Similarities between the shelf and slope communities were tested with an ANOSIM analysis, which indicated that these regions form distinct communities ($R = 0.5$, $p = .01$), with separate clusters in the species composition for shelf vs slope locations (Fig. 11). Taxa such as brittle stars, polychaete tubeworms and anemones were ubiquitous to both regions, while several other taxa were only observed on the shelf, including infaunal holothurians, colonial ascidians, sea pens, some sponges and various octocoral taxa. Sea spiders and crinoids were rare on the slope, but relatively abundant on the shelf. There were also several taxa that were absent or extremely rare on the shelf, but relatively abundant on the slope, including stony corals, bivalves, colonial anemones and bushy, non-fleshy octocorals.

5. Discussion

5.1. Extent of the former ice margin

Glacial features preserved on the outer shelf, including a GZW and a series of ridges, indicate the former expansion of the ice sheet across this shelf (Fig. 2). These features build on observations of the Sabrina shelf by Fernandez et al. (2018). The GZW observed near the shelf break marks the extent of the former grounding line within 2 km of the shelf break. The symmetrical ridges are interpreted as glacial lineations, formed parallel to flow during advance of the ice margin. The semi-transparent acoustic character of the sedimentary units, indicative of a massive structure, is consistent with deposition as a soft basal till (e.g. Livingstone et al., 2012). The north-westerly and westerly orientation and well-preserved nature of the glacial lineations is consistent with formation during expansion of the Moscow University Ice Shelf during past glaciations (Fernandez et al., 2018). The cross-cutting and more westerly orientation of the lineations indicates a secondary advance of this part of the margin.

The morphology of the Sabrina upper slope region also reflects these former ice-sheet dynamics. Elsewhere on the Antarctic margin, the formation of gullies on steep (> 10°) parts of the upper slope has been associated with previous advance of the ice sheet to the shelf margin (e.g. Dowdeswell et al., 2004; Dowdeswell et al., 2006; Gales et al.,

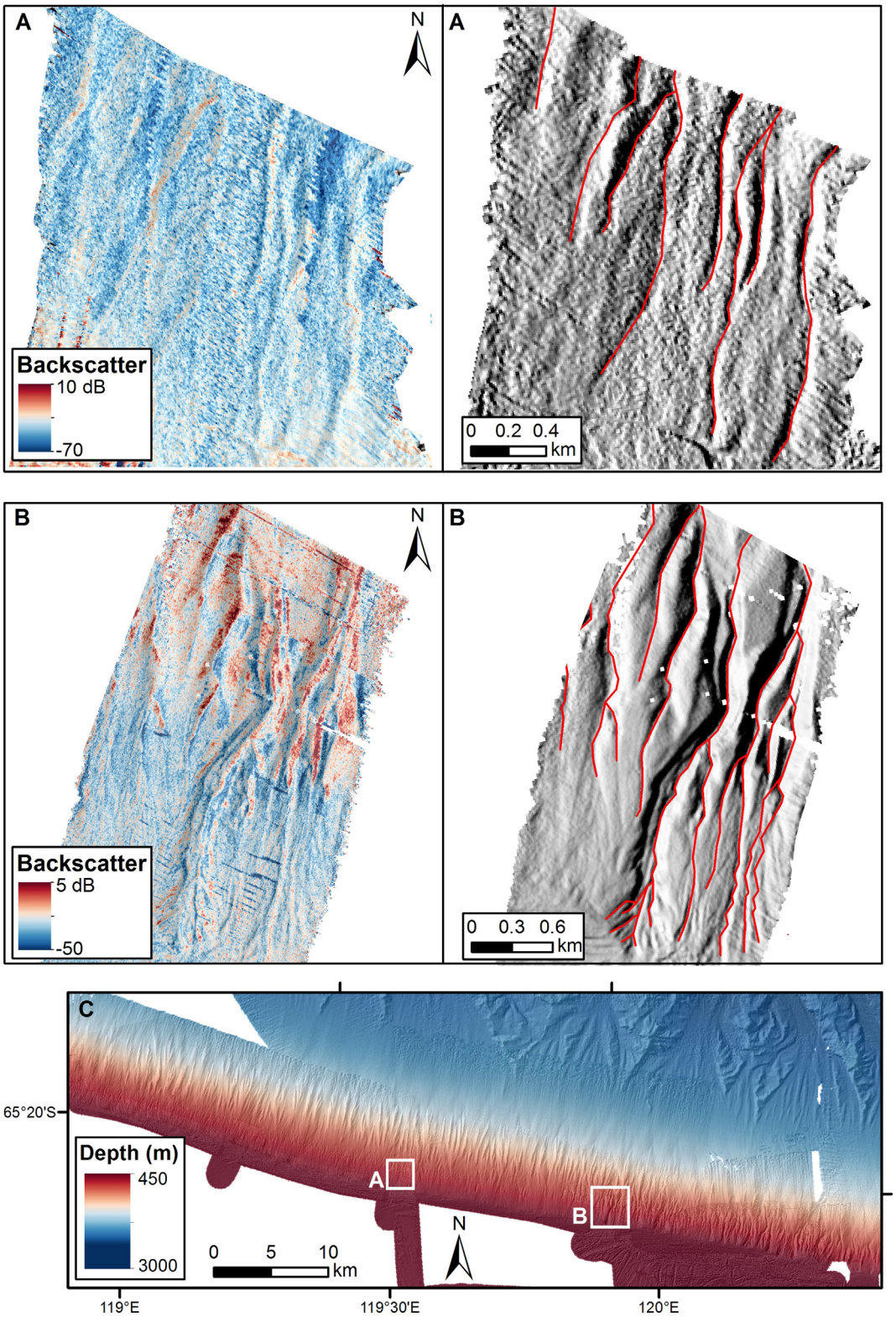

Fig. 7. Backscatter showing hard (red) to soft (blue) values on the upper slope from the EM710 sonar data (Area A and B, left-hand side). Hillshaded view (315° sun angle) showing gullies (red lines) for the same areas (right-hand side). Location of areas shown in C. (For interpretation of the references to colour in this figure legend, the reader is referred to the web version of this article.)

2013; Lowe and Anderson, 2002; Noormets et al., 2009; Ó Cofaigh et al., 2003). One of the primary mechanisms for gully formation proposed by these studies is incision by sediment-laden meltwaters released from the base of an ice sheet grounded at the shelf edge. However, the variable morphology of the gullies on the Sabrina upper slope suggests the influence of additional mechanisms, as discussed in Section 5.2.

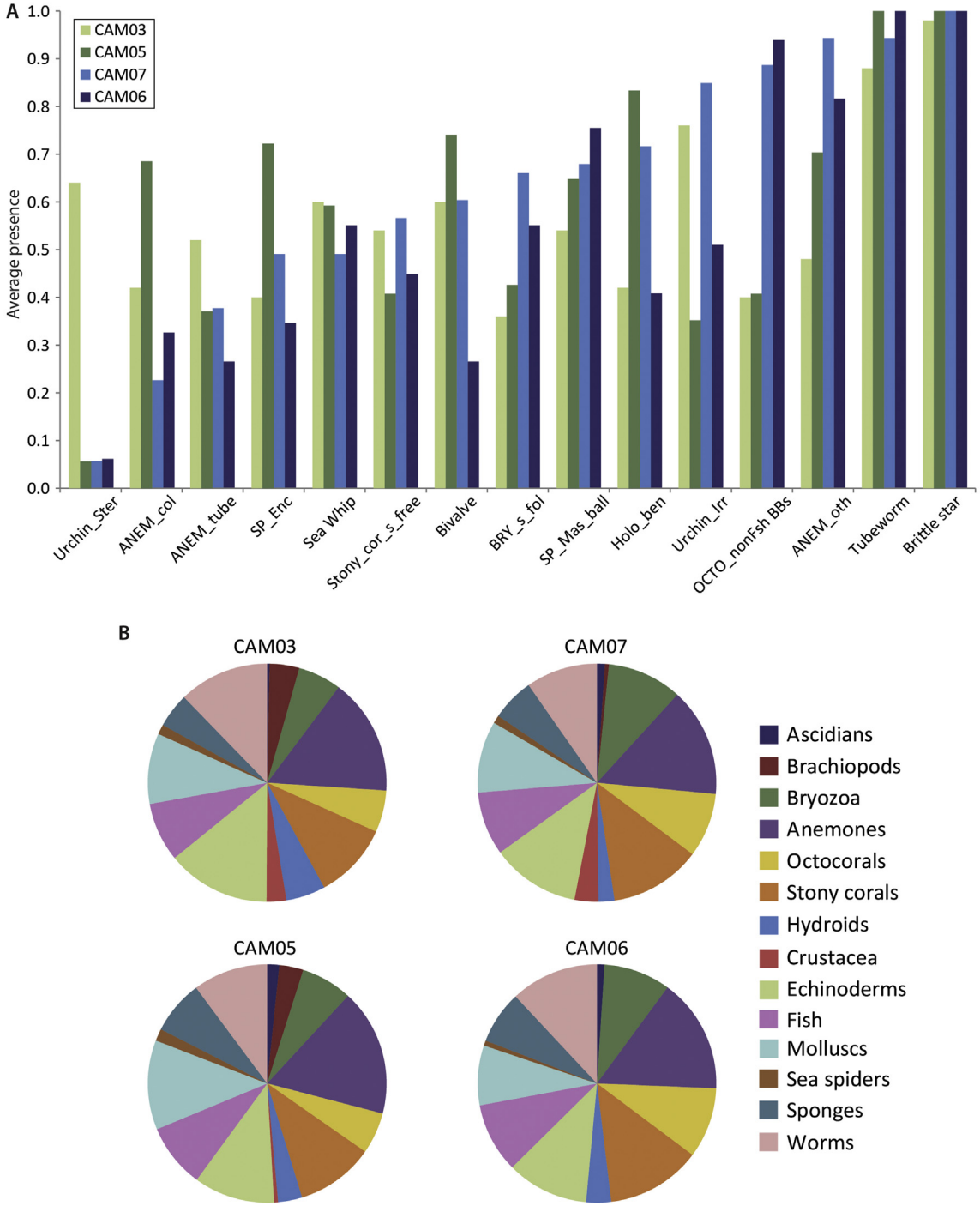

Fig. 8. Average of presence/absence data for key taxa (A) and groups of taxa (B) on each transect. Refer to Table 1 for details of number of images analysed. Urchin_Ster = urchin *Sterichinus* sp.; ANEM_col = anemone, colonial; SP_Enc = sponge, encrusting; Stony_cor_s_free = stony coral, solitary, free-living; BRY_s_fol = bryozoan, solitary, foliaceous; SP_Mas_ball = sponge, massive, ball; Holo_ben = holothurian, benthic; Urchin_Irr = urchin, irregular; OCTO_nonFsh BBs = octocoral, non-fleshy, bottle brush.

5.2. Upper slope morphology

Two morphological types of gullies form distinct groups between the eastern and western parts of the Sabrina upper slope, particularly in terms of width, depth of incision and cross-sectional shape of the gullies (see Fig. 4; Table 2). The western part of the study area exhibits lower slopes (average 9.6°) and higher proportions of U-shaped gullies than the eastern part (average slope 13.0°), suggesting a significant role for small- scale mass movements in creating the gullies, similar to processes suggested for the West Antarctic margin by Noormets et al. (2009) and Gales et al. (2012). The differences between the east and west could result from slightly higher sedimentation rates on the upper slope in the west than the east.

The occurrence of V-shaped gullies in the east, by contrast, and their incision at the shelf break, is typical of gully patterns on other margins that have been linked to submarine fluid flow (e.g. Dowdeswell et al., 2008; Micallef and Mountjoy, 2011; Gales et al., 2013). The most likely source of fluid flow is the release of sediment-laden meltwater from the base of the expanded ice sheet at the shelf edge (Anderson, 1999; Gales et al., 2013; Noormets et al., 2009; Ó Cofaigh et al., 2003; Shipp et al.,

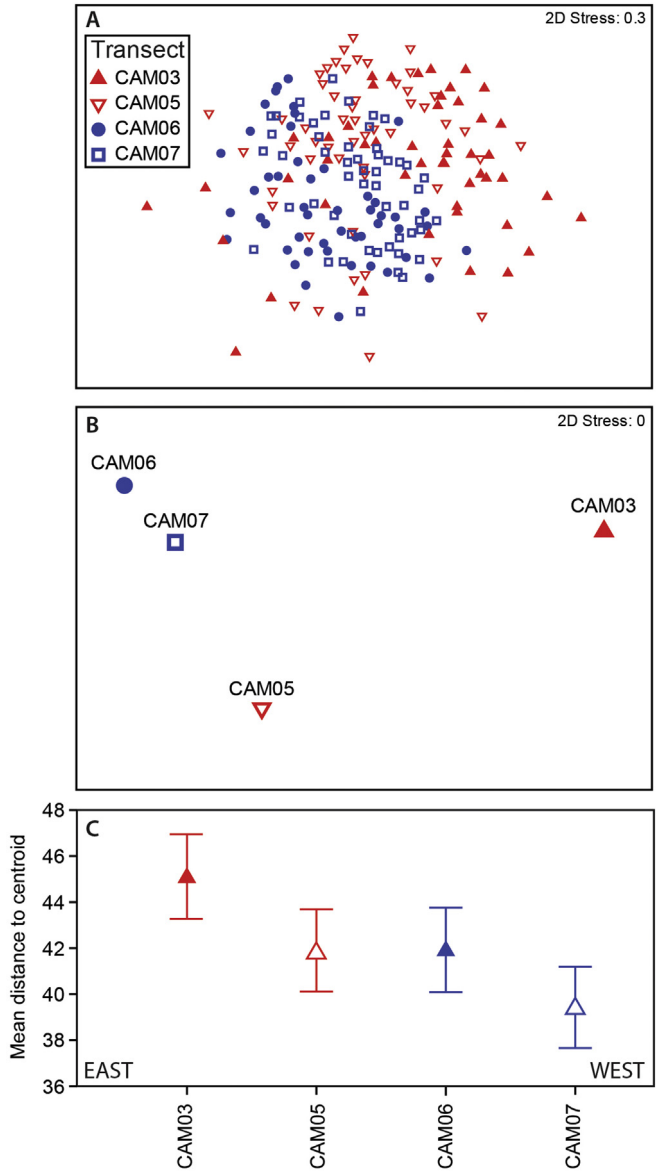

Fig. 9. (A) Non-metric multidimensional scale (MDS) plot of species resemblances, coloured according to transect. This plot shows that the species composition has considerable overlap between transects, but differences in the spread of points are observed between transects. (B) Non-metric MDS based on ANOSIM analysis showing the similarity in taxa composition between each transect. (C) Dispersion in taxa composition based on the mean distance to centroids from PERMDISP analysis. There is greater dispersion of taxa on the eastern than western transects.

Table 3
Pair-wise comparison between each transect based on PERMDISP analysis. Significant differences in dispersion of taxa are highlighted in bold.

Groups	t	P(perm)
CAM06,CAM03	2.403	**0.0203**
CAM06,CAM05	0.031268	0.9733
CAM06,CAM07	2.2437	**0.0339**
CAM03,CAM05	2.2093	**0.0393**
CAM03,CAM07	4.4646	**0.0002**
CAM05,CAM07	1.9436	0.0666

1999), which could be transferred downslope via erosive turbidity currents, developing gully networks. Additional observations of the eastern gullies are also consistent with a meltwater source. The downslope extent of the eastern gullies is relatively short, and their end point is associated with steepening slopes (see Fig. 6). These patterns are consistent with observations of turbidity current gullies on the West Antarctic Peninsula where calculations indicate a reduction in sediment load with increasing slope profile caused by the additional entrainment of seawater (Gales et al., 2013). The seawater entrainment makes the water mass more buoyant and causes it to disperse, resulting in the termination of gullies as slope angles increase. Gullies on the western side continue beyond where slope angles increase, implying that these gullies are not primarily generated by fluid flow.

Turbidity currents on the eastern side of the study area may be associated with focussing of sub-glacial meltwaters towards the edges of cross-shelf troughs, as has been inferred at the mouths of troughs in West Antarctica (Gales et al., 2013; Noormets et al., 2009). While the morphology of a cross-shelf trough is not known for the Sabrina region due to persistent sea ice cover, a deep trough has been observed on the western side of the Totten Glacier (Fig. 1; Silvano et al., 2017), and its extension to the shelf edge is consistent with past glacial advance to the shelf break (Anderson et al., 2002; Livingstone et al., 2012). The morphology of gullies on the upper slope is also consistent with the occurrence of a cross-shelf trough centred over the western part of the study area.

There is no direct evidence for meltwater activity from the morphology of the outer shelf, however, the inner shelf region adjacent to the Moscow University Ice Shelf contains meltwater channels incised into crystalline bedrock (Fernandez et al., 2018). Meltwater channels are generally less common over sedimentary substrates due to the penetration and flow of water within the subglacial till (Walder and Fowler, 1994), or the dispersal of water at the ice-sediment interface, which reworks the sediments and prevents the development of a permanent channel system (Nitsche et al., 2013). Meltwater channels are therefore rarely observed in sedimentary units on the outer shelf. The release of subglacial meltwaters onto the upper slope could initiate the formation of turbidity currents, consistent with the observed morphology of the gullies on the eastern part of the Sabrina upper slope. The erosion of gullies that initiate at the shelf break on steep (> 10°) slopes on the Antarctic Peninsula margin (Ó Cofaigh et al., 2003) and the Ross Sea (Anderson, 1999; Shipp et al., 1999) are explained by the entrainment of sediment-laden meltwaters into turbidity currents, which develop rapidly on these steep slopes.

The intense iceberg scouring adjacent to the eastern upper slope is also consistent with the large-scale gullies that occur across this part of the study region, compared to the west (Fig. 3b and c). Gales et al. (2014) found that large-scale gullies were developed adjacent to intensely scoured parts of the outer shelf due to the resuspension of sediments, which can initiate turbidity currents that further erode downslope gullies. Areas with few iceberg scours, by contrast, were incised by only small-scale gullies, as occurs on the western part of the Sabrina region.

In summary, there are key differences in gully morphology between the eastern and western parts of this area that likely reflect the balance of different processes. Based on the processes and gully morphology reported from other parts of the Antarctic margin we suggest that the differences in gully morphology may relate to sedimentation patterns, the generation of turbidity currents, and possible focussing of meltwaters. The lower slope angles on the western side likely promote deposition of unconsolidated sediments at the front of the former ice sheet. These rapidly deposited sediments are inherently unstable, resulting in small-scale mass movements, which form into relatively small, straight, U-shaped gullies initiating well below the shelf break. Higher slope angles on the eastern side create a sediment bypass zone, with sediment-laden meltwaters forming erosive turbidity currents that form larger, sinuous, often V-shaped gullies that initiate at or just below the shelf break. The termination of the eastern gullies at the point where the slope steepens (Fig. 6) is also consistent with the influence of turbidity flows.

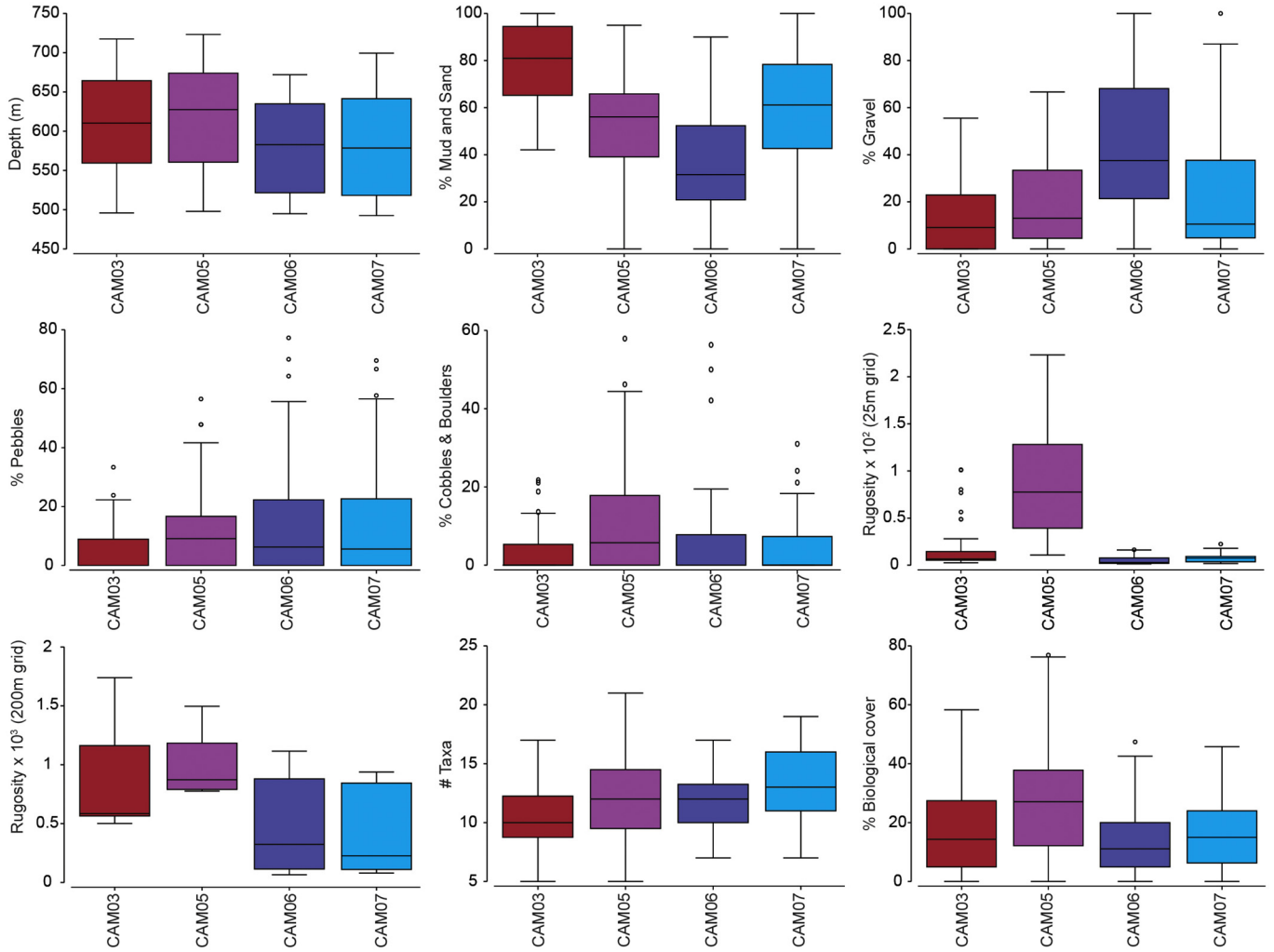

Fig. 10. Box plots showing medians, quartiles and ranges within each camera transect for key environmental variables, as well as the number of taxa and the biological cover.

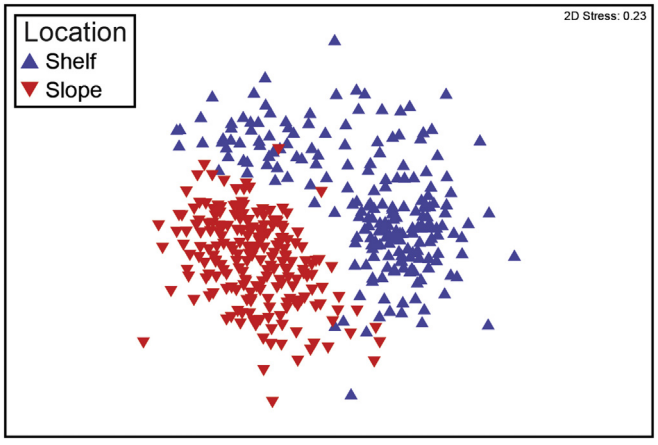

Fig. 11. Non-metric MDS plot showing close similarity of taxa within shelf and slope communities, with distinct separation in composition of benthic taxa between these regions.

Higher backscatter values in the base of the gullies indicates coarser sediment, implying that these channels are being flushed by relatively high-energy currents in either recent or present times (see also Dowdeswell et al., 2008; Noormets et al., 2009). Seafloor images support the presence of coarse-grained sediments in the base of the channels, with average gravel cover ranging from 15 to 43% of the image area.

5.3. Influence of gully type on seafloor biota

The composition of seafloor biota did not vary significantly between the four gullies surveyed, suggesting a relatively homogeneous upper slope community that is largely unrestricted by the dispersal of taxa over these scales. However, differences were observed in the beta-diversity of the seafloor communities, with decreasing beta-diversity evident from east to west. This pattern in beta-diversity is broadly consistent with the east to west change from more rugged to smoother gully types (Fig. 12). The broad association between beta-diversity and gully type may reflect a greater heterogeneity of habitats in the rugged gullies, allowing a broader range in the structure of the benthic community. Rugged gullies will tend to have steeper side walls, greater surface area, more variable substrate types and may be associated with enhanced current flows and nutrient delivery than smoother gullies, consistent with observations in slope canyons (e.g. McClain and Barry, 2010; Schlacher et al., 2007; Vetter et al., 2010). Higher beta-diversity in benthic macrofauna has also been associated with increased environmental heterogeneity on the Norwegian continental shelf (Anderson et al., 2006) and at local scales on the Ross Sea coast, Antarctica (Thrush et al., 2010). Therefore, understanding the heterogeneity of habitat features is important for understanding local-scale

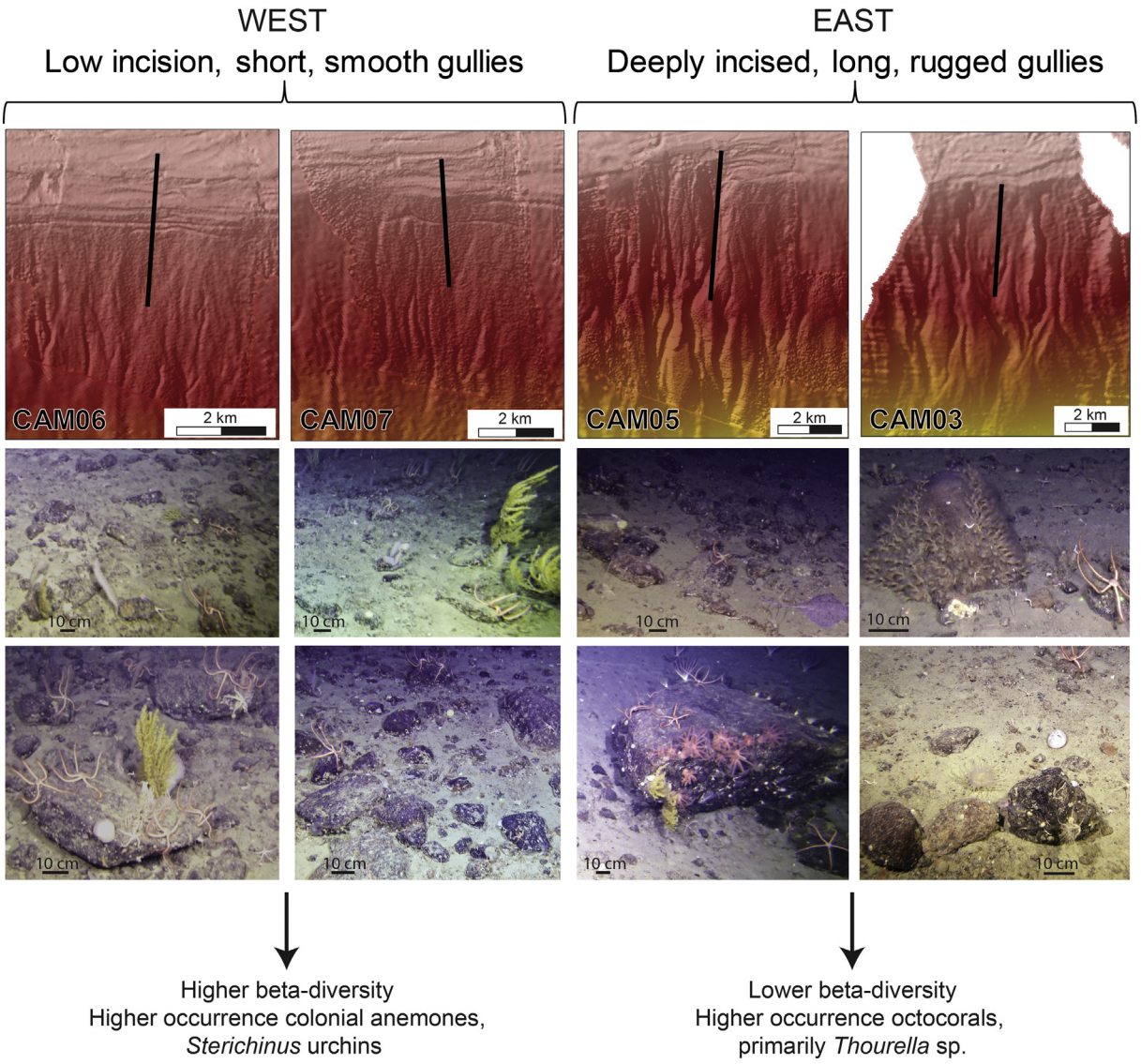

Fig. 12. Summary gully types and biota across the four transects. The top seafloor image for CAM03 illustrates abundant colonial anemones covering a boulder, while CAM05 also contains sponges, crinoids, soft-corals and bivalves. CAM06 and CAM07 both contain abundant soft corals, including the simple bottle-brush form, *Thourella* sp. and brittle stars.

diversity patterns and community structure.

The importance of the continental slope as a distinct habitat has been the focus of previous studies that have sought to understand connectivity between Antarctic shelf, slope and abyssal faunas (Barnes and Kuklinski, 2010; Kaiser et al., 2011; Linse et al., 2013; Neal et al., 2018; Pabis et al., 2015). Determining the degree to which benthic communities in these regions are distinct has important implications for assessing conservation priorities, and for understanding colonisation and evolutionary history, particularly the potential of the slope and abyss to act as a source for shelf recolonisation following glaciations (e.g. Kaiser et al., 2011; Thatje et al., 2005). However, as the present and previous studies show (Dowdeswell et al., 2004; Ó Cofaigh et al., 2003), glaciations are thought to induce turbid flow of glaciogenic debris and erosion of the slope, making this a hostile environment for benthic biota during glacial periods. It is possible that the shelf biota were recolonised from shelf refugia and, perhaps, abyssal environments (Thatje et al., 2005). The comparison between shelf and slope biota in this study advances our understanding of the degree to which these communities may be connected at a taxa level, by contrasting communities imaged within the same depth range (500–725 m) on the upper slope and the adjacent continental shelf (Post et al., 2017). The clear distinction between the shelf and slope communities in the Sabrina region suggests little connection between these benthic communities, consistent with that observed for specific taxa on other parts of the Antarctic margin (e.g. Weddell Sea: Barnes and Kuklinski, 2010; Kaiser et al., 2011; Ross Sea: Pabis et al., 2015; Amundsen Sea and Scotia Sea: Neal et al., 2018; Amundsen Sea: Linse et al., 2013).

The results from this comparison illustrate the distinct differences in environmental features (with the exception of depth) between the slope and shelf environments, which we believe limits the distribution of taxa across these environments today, during interglacial periods, and presumably quite severely during glaciations. The shelf and slope are distinct in their seafloor morphology, stability, substrates and productivity regimes. The slope is a dynamic area, at times impacted by turbidite flows, but also associated with the downslope transport of phytodetritus, which can enhance the biomass and abundance of seafloor fauna (Schlacher et al., 2007). On the Sabrina shelf, by contrast, phytoplankton blooms typically occur during a period of < 6 weeks in the year (Johnson et al., 2013), generating an extremely short seasonal flux of detritus to the seafloor. The observation of suspension feeding by brittle stars on the slope (Fig. 12), compared to those on the shelf that adopted other feeding strategies (Fig. 4 in Post et al., 2017), may reflect

a higher advected food supply within slope gullies (e.g. Calero et al., 2018). Substrates on the Sabrina shelf are also more uniform than those on the adjacent slope. At the depths analysed here (500–725 m), the shelf substrates are almost exclusively sand/mud (Post et al., 2017), whereas the substrates imaged on the slope are much more variable, ranging from mud/sand to cobbles and boulders (Fig. 10). These factors create distinct habitat characteristics between the shelf and slope in this region. We therefore argue that conservation strategies need to consider slope and shelf communities as distinct and equally important components of the Antarctic ecosystem.

6. Conclusion

Variations in upper slope gully morphology reflect differences in the depositional history associated with the former ice-sheet dynamics along this part of the East Antarctic margin. Based on the characteristics of the gullies, we suggest that lower slope angles of the upper slope in the western part of the region may have promoted rapid sediment deposition and subsequent mass wastage, creating gullies that are typically shallow, straight, long and U-shaped. Higher slope values in the east may have resulted in the formation of erosive turbidity currents during glacial expansion of the ice sheet to the shelf edge and release of sediment-laden basal meltwaters. Fluid flows typically generate gullies that initiate at or near the shelf break with V-shaped profiles, a relatively short downslope extent and high sinuosity, which appear typical for gullies on the eastern part of this margin. The differences in gully morphology are associated with variations in the structure of seafloor communities, with higher beta-diversity in the more rugged gullies consistent with the greater heterogeneity of habitats available within these more complex gully environments. The distinct difference between the upper slope communities and those of the adjacent continental shelf, reflects significant differences in habitat between the upper slope and the shelf, which limits the distribution of taxa across these environments. The upper slope region is a unique environment in its formation and processes, which influences the distribution and composition of benthic communities. Conservation strategies therefore need to consider slope and shelf communities as distinct and equally important components of the Antarctic ecosystem.

Data availability

All voyage data, including multibeam bathymetry, is available from: https://www.cmar.csiro.au/data/trawler/survey_details.cfm?survey=IN2017_V01

Colour corrected still images are archived at: http://dapds00.nci.org.au/thredds/catalog/fk1/IN2017_V01_Sabrina_Seafloor/catalog.html

Still image annotations are available from: https://data.aad.gov.au/metadata/records/AAS_4333_IN2017_V01_seafloor_imagery_annotations

Acknowledgements

We thank the Marine National Facility (MNF), the IN2017-V01 scientific party, MNF support staff and ASP crew members led by Capt. M. Watson for their help and support on board the RV *Investigator*. In particular, we thank Rod Palmer and Nicole Morgan for assistance with the deployment of the Deep Tow camera, Tara Martin for assistance with multibeam bathymetry acquisition and processing and Doug Thost for his support as voyage manager. We also thank Jacob Martin for assistance mapping gullies and Alistair Deane for assistance with image analysis. Ari Friedmann is thanked for his assistance in setting up the images for analysis in Squidle+ and Adam Smith for assistance with statistical analyses in PRIMER 7. We thank Rachel Przeslawski, Nadege Rollet, Amy Leventer, Sergio Rossi and an anonymous reviewer for constructive reviews of an earlier version of this manuscript. All data and samples acquired on the voyage are made publicly available in accordance with MNF Policy and are available via the Australian Antarctic Data Centre or the MNF website. This project is supported through funding from the Australian Government's Australian Antarctic Science Grant Program (AAS #4333). ALP and AGC publish with the permission of the Chief Executive Officer, Geoscience Australia.

References

Aitken, A., Roberts, J., van Ommen, T., Young, D., Golledge, N., Greenbaum, J., Blankenship, D., Siegert, M., 2016. Repeated large-scale retreat and advance of Totten Glacier indicated by inland bed erosion. Nature 533, 385–389.

Althaus, F., Hill, N., Ferrari, R., Edwards, L., Przeslawski, R., Schönberg, C.H.L., Stuart-Smith, R., Barrett, N., Edgar, G., Colquhoun, J., Tran, M., Jordan, A., Rees, T., Gowlett-Holmes, K., 2015. A standardised vocabulary for identifying benthic biota and substrata from underwater imagery: the CATAMI classification scheme. PLoS One 10, e0141039.

Amblas, D., Dowdeswell, J.A., 2018. Physiographic influences on dense shelf-water cascading down the Antarctic continental slope. Earth Sci. Rev. 185, 887–900.

Anderson, J.B., 1999. Antarctic Marine Geology. Cambridge University Press, Cambridge.

Anderson, J.B., Shipp, S.S., Lowe, A.L., Wellner, J.S., Mosola, A.B., 2002. The Antarctic ice sheet during the Last Glacial Maximum and its subsequent retreat history: a review. Quat. Sci. Rev. 21, 49–70.

Anderson, M.J., Ellingsen, K.E., McArdle, B.H., 2006. Multivariate dispersion as a measure of beta diversity. Ecol. Lett. 9, 683–693.

Armand, L., O'Brien, P., Armbrecht, L., Baker, H., Caburlotto, A., Connell, T., Cotterle, D., Duffy, M., Edwards, S., Evangelinos, D., Fazey, J., Flint, A., Focardi, A., Gifford, S., Holder, L., Hughes, P., Lawler, K.-A., Lieser, J., Leventer, A., Lewis, M., Martin, T., Morgan, N., López Quirós, A., Malakoff, K., Noble, T., Opdyke, B., Palmer, R., Perera, R., Pirotta, V., Post, A., Romeo, R., Simmons, J., Thost, D., Tynan, S., Young, A., 2018. Interactions of the Totten Glacier With the Southern Ocean Through Multiple Glacial Cycles (IN2017-V01): Post-survey Report. Research School of Earth Sciences, The Australian National University, Canberra, ACT, pp. 143.

Arndt, J.E., Schenke, H.W., Jakobsson, M., Nitsche, F.O., Buys, G., Goleby, B., Rebesco, M., Bohoyo, F., Hong, J., Black, J., Greku, R., Udintsev, G., Barrios, F., Reynoso-Peralta, W., Taisei, M., Wigley, R., 2013. The International Bathymetric Chart of the Southern Ocean (IBCSO) Version 1.0 – a new bathymetric compilation covering circum-Antarctic waters. Geophys. Res. Lett. 311–317.

Barnes, D.K.A., Kuklinski, P., 2010. Bryozoans of the Weddell Sea continental shelf, slope and abyss: did marine life colonize the Antarctic shelf from deep water, outlying islands or in situ refugia following glaciations? J. Biogeogr. 37, 1648–1656.

Barnes, P.W., Lien, R., 1988. Icebergs rework shelf sediments to 500 m off Antarctica. Geology 16, 1130–1133.

Bindoff, N.L., Rosenberg, M.A., Warner, M.J., 2000. On the circulation of water masses over the Antarctic continental slope and rise between 80 and 150°E. Deep-Sea Res. II 47, 2299–2326.

Calero, B., Ramos, A., Ramil, F., 2018. Distribution of suspension-feeder brittle stars in the Canary current upwelling ecosystem (Northwest Africa). Deep-Sea Res. I Oceanogr. Res. Pap. 142, 1–15.

Carroll, A., Althaus, F., Beaman, R., Friedman, A., Ierodiaconou, D., Ingleton, T., Jordan, A., Linklater, M., Monk, J., Post, A., Przeslawski, R., Smith, J., Stowar, M., Tran, M., Tyndall, A., 2018. Marine sampling field manual for towed underwater camera systems. In: Przeslawski, R., Foster, S. (Eds.), In Field Manuals for Marine Sampling to Monitor Australian Waters. National Environmental Science Programme (NESP), pp. 131–152.

Clarke, K.R., Gorley, R.N., Somerfield, P.J., Warwick, R.M., 2014. Change in Marine Communities: An Approach to Statistical Analysis and Interpretation, 3rd edition. PRIMER-E, Plymouth.

Dowdeswell, J., Cofaigh, C., Pudsey, C., 2004. Continental slope morphology and sedimentary processes at the mouth of an Antarctic palaeo-ice stream. Mar. Geol. 204, 203–214.

Dowdeswell, J.A., Evans, J., Ó Cofaigh, C., Anderson, J.B., 2006. Morphology and sedimentary processes on the continental slope off Pine Island Bay, Amundsen Sea, West Antarctica. Geol. Soc. Am. Bull. 118, 606–619.

Dowdeswell, J.A., Cofaigh, C., Noormets, R., Larter, R.D., Hillenbrand, C.D., Benetti, S., Evans, J., Pudsey, C.J., 2008. A major trough-mouth fan on the continental margin of the Bellingshausen Sea, West Antarctica: the Belgica Fan. Mar. Geol. 252, 129–140.

Fernandez, R., Gulick, S., Domack, E., Montelli, A., Leventer, A., Shevenell, A., Frederick, B., 2018. Past ice stream and ice sheet changes on the continental shelf off the Sabrina Coast, East Antarctica. Geomorphology 317, 10–22.

Fofonoff, N.P., Millard Jr, R., 1983. Algorithms for the computation of fundamental properties of seawater. In: UNESCO Technical papers in marine science 44.

Gales, J., Larter, R., Mitchell, N., Hillenbrand, C.D., Østerhus, S., Shoosmith, D., 2012. Southern Weddell Sea shelf edge geomorphology: implications for gully formation by the overflow of high-salinity water. J. Geophys. Res. Earth Surf. 117.

Gales, J., Leat, P., Larter, R., Kuhn, G., Hillenbrand, C.-D., Graham, A., Mitchell, N., Tate, A., Buys, G., Jokat, W., 2014. Large-scale submarine landslides, channel and gully systems on the southern Weddell Sea margin, Antarctica. Mar. Geol. 348, 73–87.

Gales, J.A., Larter, R.D., Mitchell, N.C., Dowdeswell, J.A., 2013. Geomorphic signature of Antarctic submarine gullies: implications for continental slope processes. Mar. Geol. 337, 112–124.

Gulick, S.P.S., Shevenell, A.E., Montelli, A., Fernandez, R., Smith, C., Warny, S., Bohaty, S.M., Sjunneskog, C., Leventer, A., Frederick, B., Blankenship, D.D., 2017. Initiation

and long-term instability of the East Antarctic ice sheet. Nature 552, 225.
Jansen, J., Hill, N.A., Dunstan, P.K., McKinlay, J., Sumner, M.D., Post, A.L., Eléaume, M.P., Armand, L.K., Warnock, J.P., Galton-Fenzi, B.K., Johnson, C.R., 2018. Abundance and richness of key Antarctic seafloor fauna correlates with modelled food availability. Nature Ecol. Evol. 2, 71–80.
Johnson, R., Strutton, P.G., Wright, S.W., McMinn, A., Meiners, K.M., 2013. Three improved satellite chlorophyll algorithms for the Southern Ocean. J. Geophys. Res. Oceans 118, 3694–3703.
Kaiser, S., Griffiths, H.J., Barnes, D.K.A., Brandão, S.N., Brandt, A., O'Brien, P.E., 2011. Is there a distinct continental slope fauna in the Antarctic? Deep-Sea Res. II Top. Stud. Oceanogr. 58, 91–104.
Kuvaas, B., Kristoffersen, Y., 1991. The Crary Fan: a trough-mouth fan on the Weddell Sea continental margin, Antarctica. Mar. Geol. 97, 345–362.
Linse, K., Griffiths, H.J., Barnes, D.K.A., Brandt, A., Davey, N., David, B., De Grave, S., d'Udekem d'Acoz, C., Eléaume, M., Glover, A.G., Hemery, L.G., Mah, C., Martín-Ledo, R., Munilla, T., O'Loughlin, M., Pierrat, B., Saucède, T., Sands, C.J., Strugnell, J.M., Enderlein, P., 2013. The macro- and megabenthic fauna on the continental shelf of the eastern Amundsen Sea. Antarctica. Cont. Shelf Res. 68, 80–90.
Livingstone, S.J., Ó Cofaigh, C., Stokes, C.R., Hillenbrand, C.-D., Vieli, A., Jamieson, S.S.R., 2012. Antarctic palaeo-ice streams. Earth Sci. Rev. 111, 90–128.
Lowe, A.L., Anderson, J.B., 2002. Reconstruction of the West Antarctic ice sheet in Pine Island Bay during the Last Glacial Maximum and its subsequent retreat history. Quat. Sci. Rev. 21, 1879–1897.
Massom, R.A., Harris, P.T., Michael, K.J., Potter, M.J., 1998. The distribution and formative processes of latent-heat polynyas in East Antarctica. Ann. Glaciol. 27, 420–426.
McClain, C.R., Barry, J.P., 2010. Habitat heterogeneity, disturbance, and productivity work in concert to regulate biodiversity in deep submarine canyons. Ecology 91, 964–976.
Micallef, A., Mountjoy, J.J., 2011. A topographic signature of a hydrodynamic origin for submarine gullies. Geology 39, 115–118.
Neal, L., Linse, K., Brasier, M.J., Sherlock, E., Glover, A.G., 2018. Comparative marine biodiversity and depth zonation in the Southern Ocean: evidence from a new large polychaete dataset from Scotia and Amundsen seas. Mar. Biodivers. 48, 581–601.
Nitsche, F.O., Gohl, K., Larter, R.D., Hillenbrand, C.-D., Kuhn, G., Smith, J., Jacobs, S., Anderson, J., Jakobsson, M., 2013. Paleo ice flow and subglacial meltwater dynamics in Pine Island Bay, West Antarctica. Cryosphere 7, 249–262.
Nitsche, F.O., Porter, D., Williams, G., Cougnon, E.A., Fraser, A.D., Correia, R., Guerrero, R., 2017. Bathymetric control of warm ocean water access along the East Antarctic margin. Geophys. Res. Lett. 44, 8936–8944.
Noormets, R., Dowdeswell, J.A., Larter, R.D., Ó Cofaigh, C., Evans, J., 2009. Morphology of the upper continental slope in the Bellingshausen and Amundsen Seas – implications for sedimentary processes at the shelf edge of west Antarctica. Mar. Geol. 258, 100–114.
Ó Cofaigh, C., Taylor, J., Dowdeswell, J.A., Pudsey, C.J., 2003. Palaeo-ice streams, trough mouth fans and high-latitude continental slope sedimentation. Boreas 32, 37–55.
O'Brien, P.E., Post, A.L., S., E., Martin, T., Armand, L.K., Caburlotto, Donda, F., Leitchenkov, G., Romeo, R., Duffy, M., Evangelios, D., Holder, L., Lopez-Quiros, A., submitted. in review. Continental slope geomorphology seaward of the Totten Glacier, East Antarctica. Marine Geology.
Pabis, K., Jóźwiak, P., Lörz, A.-N., Schnabel, K., Błażewicz-Paszkowycz, M., 2015. First insights into the deep-sea tanaidacean fauna of the Ross Sea: species richness and composition across the shelf break, slope and abyss. Polar Biol. 38, 1429–1437.
Pattyn, F., Van Huele, W., 1998. Power law or power flaw? Earth Surf. Process. Landf. 23, 761–767.
Post, A., O'Brien, P.E., Armand, L.K., Carroll, A., 2019. Seafloor Image Annotations From the Sabrina Upper Slope, East Antarctica. Australian Antarctic Data Centrehttps://doi.org/10.26179/5caed60a7b076.
Post, A.L., O'Brien, P.E., Beaman, R.J., Riddle, M.J., De Santis, L., 2010. Physical controls on deep-water coral communities on the George V Land slope, East Antarctica. Antarct. Sci. 22, 371–378 (doi:310.1017/S0954102010000180).
Post, A.L., Lavoie, C., Domack, E.W., Leventer, A., Shevenell, A., Fraser, A.D., 2017. Environmental drivers of benthic communities and habitat heterogeneity on an East Antarctic shelf. Antarct. Sci. 29, 17–32.
Prothro, L.O., Simkins, L.M., Majewski, W., Anderson, J.B., 2018. Glacial retreat patterns and processes determined from integrated sedimentology and geomorphology records. Mar. Geol. 395, 104–119.
Schlacher, T.A., Schlacher-Hoenlinger, M.A., Althaus, F., Hooper, J.N.A., Kloser, R., 2007. Richness and distribution of sponge megabenthos in continental margin canyons off southeastern Australia. Mar. Ecol. Prog. Ser. 340, 73–88.
Shipp, S., Anderson, J., Domack, E., 1999. Late Pleistocene–Holocene retreat of the West Antarctic Ice-Sheet system in the Ross Sea: part 1—geophysical results. Geol. Soc. Am. Bull. 111, 1486–1516.
Silvano, A., Rintoul, S.R., Herraiz-Borreguero, L., 2017. Distribution of water masses and meltwater on the continental shelf near the Totten and Moscow University ice shelves. J. Geophys. Res. Oceans 29, 130–143.
Strahler, A.N., 1957. Quantitative analysis of watershed geomorphology. Trans. Am. Geophys. Union 8, 913–920.
Thatje, S., Hillenbrand, C.D., Larter, R., 2005. On the origin of Antarctic marine benthic community structure. Trends Ecol. Evol. 20, 534–540.
Thrush, S.F., Hewitt, J.E., Cummings, V.J., Norkko, A., Chiantore, M., 2010. β-Diversity and species accumulation in Antarctic coastal benthos: influence of habitat, distance and productivity on ecological connectivity. PLoS One 5, e11899.
Vetter, E.W., Smith, C.R., De Leo, F.C., 2010. Hawaiian hotspots: enhanced megafaunal abundance and diversity in submarine canyons on the oceanic islands of Hawaii. Mar. Ecol. 31, 183–199.
Walder, J.S., Fowler, A., 1994. Channelized subglacial drainage over a deformable bed. J. Glaciol. 40, 3–15.
Whittaker, R.H., 1960. Vegetation of the Siskiyou mountains, Oregon and California. Ecol. Monogr. 30, 279–338.
Whittaker, R.H., 1972. Evolution and measurement of species diversity. Taxon 213–251.
Williams, G.D., Meijers, A.J.S., Poole, A., Mathiot, P., Tamura, T., Klocker, A., 2011. Late winter oceanography off the Sabrina and BANZARE coast (117–128°E), East Antarctica. Deep-Sea Res. II Top. Stud. Oceanogr. 58, 1194–1210.
Wright, D.J., Pendleton, M., Boulware, J., Walbridge, S., Gerlt, B., Eslinger, D., Sampson, D., Huntley, E., 2012. ArcGIS Benthic Terrain Modeler (BTM), v. 3.0. Environmental Systems Research Institute, NOAA Coastal Services Center, Massachusetts Office of Coastal Zone Management Available online at. http://esriurl.com/5754.
Young, D.A., Wright, A.P., Roberts, J.L., Warner, R.C., Young, N.W., Greenbaum, J.S., Schroeder, D.M., Holt, J.W., Sugden, D.E., Blankenship, D.D., van Ommen, T.D., Siegert, M.J., 2011. A dynamic early East Antarctic Ice Sheet suggested by ice-covered fjord landscapes. Nature 474, 72–75.